Reducing CO_2 to Methanol using Frustrated Lewis Pairs: On the Mechanism of Phosphine-Borane Mediated Hydroboration of CO_2

Marc-André Courtemanche,[a] Marc-André Légaré,[a] Laurent Maron[b] and Frédéric-Georges Fontaine*[a]*

[a] Département de Chimie, Université Laval, 1045 Avenue de la Médecine, Québec (Québec), Canada, G1V 0A6

[b] Université de Toulouse, INSA, UPS, LCPNO, CNRS, UMR 5215 CNRS-UPS-INSA, 135 avenue de Rangueil, Toulouse, France

E-mails: frederic.fontaine@chm.ulaval.ca and laurent.maron@irsamc.ups-tlse.fr

This is the peer reviewed version of the following article: [Reducing CO2 to Methanol using Frustrated Lewis Pairs: On the Mechanism of Phosphine-Borane Mediated Hydroboration of CO2, J. Am. Chem. Soc. 2014, 136, 10708−10717], which has been published in final form at [10.1021/ja5047846].

Abstract

The full mechanism for the hydroboration of CO_2 by highly active ambiphilic organocatalyst 1-Bcat-2-PPh_2−C_6H_4 (cat = catechol) was determined using computational and experimental methods. The intramolecular Lewis pair was shown to be involved in every step of the stepwise reduction. Contrasting with traditional FLP systems, the lack of steric hindrance around the Lewis basic fragment allows activation of the reducing agent while moderate Lewis acidity/basicity at the active centers promotes catalysis by releasing the reduction products. Simultaneous activation of both the reducing agent and carbon dioxide is the key to efficient catalysis in every reduction step.

Introduction

The general concern over the increase of the CO_2 concentration in the atmosphere and its influence on climate change has led to several worldwide initiatives to control the emissions of this green-house gas. Although several carbon capture technologies have been developed, the possibility of using CO_2 as a C-1 feedstock to synthesize valuable chemicals could be an important financial incentive for reducing CO_2 emissions.[1] For these reasons, carbon dioxide transformation has attracted much scientific attention over the past decade.[2] Of particular interest and at the core of the methanol economy is the transformation of CO_2 into high hydrogen content hydrocarbons since such technology could help generate "green" energy vectors that are needed on a global scale to replace fossil fuels.[3] Although most of the reported systems use heterogeneous catalysts, some homogeneous transition-metal based catalytic systems have been developed for the reduction of CO_2 to formic acid,[4] formate,[5] formaldehyde,[6] methanol,[7] methane[8] and acetals.[9]

Organocatalysts, as species not comprised of transition metals, are still scarce in the field of CO_2 functionalization to valuable chemicals.[10] Notable systems include highly Lewis acidic aluminum species[11] and silyl cations[12] which have been shown to reduce CO_2 with low selectivity to mixtures of products comprising methane, methanol and a number of alkylation by-products. Pioneering work by Stephan and Erker demonstrated the capacity of FLPs (Frustrated Lewis Pairs) to bind carbon dioxide which led to the subsequent discovery of a number of ambiphilic systems capable of stoichiometric fixation.[13] However, except for the reduction of CO_2 to CO by carbodiphosphoranes,[14] no other catalytic reduction of CO_2 was reported for these systems. The $PMes_3/AlX_3$ (X=Cl, Br, C_6F_5) FLP mediated the stoichiometric reduction of CO_2 using $NH_3{\bullet}BH_3$, but the system had to be destroyed by hydrolysis in order to free the reduced

methoxide fragment and generate methanol.[15] Piers also developed an FLP based catalytic reduction of CO_2 to methane by using hydrosilanes, albeit with limited turnovers.[16] Zhang *et al.* reported that N-heterocyclic carbenes could be used as catalysts to reduce CO_2 to methanol in the presence of hydrosilanes with a turn-over frequency (TOF) of 25 h^{-1} at room temperature.[17] Recently, Cantat demonstrated that some nitrogen bases, such as guanidines and amidines, could be used as catalysts for the reduction of CO_2 to formamide using hydrosilanes[18] or to methoxyboranes using 9-borabicyclo[3.3.1]nonane (9-BBN) and HBcat (cat = catechol).[19] Stephan also reported that phosphines could catalyze the reduction of CO_2 to methoxyboranes using 9-BBN as the reducing agent.[20]

Our group recently reported that organocatalyst 1-Bcat-2-PPh_2−C_6H_4 (**1**), which can also be generated by the addition of HBcat to precatalyst Al(2-PPh_2-C_6H_4)$_3$,[21] is highly active for the hydroboration of CO_2 to methoxyboranes, species that can be readily hydrolyzed to methanol, using a variety of hydroboranes.[22] Using catecholborane or high hydrogen containing BH_3•SMe_2, a turn-over frequency (TOF) of 973 h^{-1} and turn-over numbers (TON) over 2950 were observed at a temperature of 70°C. In a recent contribution, Stephan *et al.* reported a similar ambiphilic system to be catalytically active in the hydroboration of CO_2.[23] Both of these systems have in common the weak Lewis acidity of the borane compared to the strong Lewis acids normally used in classical FLP systems. Understanding the fundamental process of this catalytic system and identifying the important reaction intermediates is therefore of prime importance in order to unveil the full potential of ambiphilic molecules and frustrated Lewis pairs as efficient catalysts. In order to determine the true role of the catalyst in every step of the reduction process, a thorough computational study has been carried out and complemented by experimental studies. Herein, we report the full mechanism for the first metal-free catalytic hydroboration of CO_2 to

methoxyboranes. A closer look at the critical steps of the reaction underlines some of the key aspects of the mechanism and offers an unprecedented insight and a novel way to approach ambiphilic molecule and FLP-mediated catalysis.

Computational details

All the calculations were performed on the full structures of the reported compounds. Calculations were performed with the GAUSSIAN 03 and GAUSSIAN 09 suite of programs.[24,25] While the wB97XD functional[26] was qualified as promising by Grimme[27] and was used to accurately describe the mechanism of FLP mediated hydrogenation of alkynes[28], its use for the modelization of **1** showed a very different geometry than the reported crystal structure.[21] Based on the accurate description of **1** with respect to the reported structure, the B3PW91[29] functional was used in combination with the 6-31G** basis set for B, C, H, and O atoms[30] and the SDD basis set with an additional polarization function (one d function with a 0.34 exponent and a 1.0 contraction coefficient) for the P atom.[31] The transition states were located and confirmed by frequency calculations (single imaginary frequency). Intrinsic reaction coordinate calculations (IRC) have been performed to confirm the link between the transition states and the reactants/products. The stationary points were characterized as minima by full vibration frequencies calculations (no imaginary frequency). All geometry optimizations were carried out without any symmetry constraints. The energies were then refined by single point calculations to include dispersion at the B97D/6-31G** level of theory.[32] The energies were further refined by single point calculations to account for solvent effects using the SMD solvation model[33] with benzene, the experimental solvent. The difference between the energies with or without the solvation model can be found in the ESI. Since the entropic contribution in solution cannot be accurately predicted by standard quantum mechanical calculations and are often greatly

overestimated,[34] it was shown that enthalpy values are a better approximation. Thus, the energies are reported in terms of enthalpy with the free energy reported between parentheses. Bond rotations and their associated transition states were not calculated as it is clear that their energy will be much lower than the energy barriers associated with the reduction steps in such a system and are therefore trivial. All structures with their associated free enthalpy and Gibbs free energies as well as their cartesian coordinates are fully detailed in the supporting information.

Results and discussion

At this point, it is very important to mention that the entropic contributions for gas phase calculations have been shown to be overestimated by 50-60% for a two component reaction.[35] Thus, for the majority of the reported reactions (where three components come together), the entropic contribution, and therefore the free energy, is expected to be greatly overestimated. Some strategies have been used to better estimate the entropic contribution, notably by performing the vibrational analysis at up to 1324 atm[36] to account for better entropy correction, but for this study the free energies are provided without any correction. Even though entropic contributions are important and cannot be neglected, the enthalpy values provide more accurate comparisons for similar intermediates.

The hydroboration of carbon dioxide to methoxyboranes is a stepwise process that occurs through three subsequent reduction processes. First, CO_2 is reduced to a formatoborate, which is then reduced to formaldehyde. Finally, the formaldehyde is reduced to methoxyboranes (Scheme 1). The upcoming sections will consider these three reductions steps one by one in order to simplify the discussion.

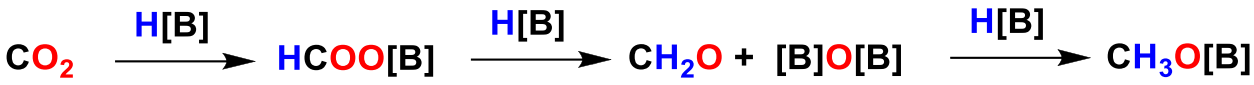

Scheme 1. Schematic representation of the stepwise hydroboration of CO_2 to methoxyboranes using hydroboranes (H[B])

First reduction step: CO_2 to HCOOBcat

As expected, the direct reduction of carbon dioxide by catecholborane (HBcat) is kinetically forbidden as the associated transition state **TS1** was located at +34.2 *(+47.7)* kcal.mol^{-1} higher than the reactants. Experimental results support this hypothesis as heating HBcat in the presence of 1 atm of CO_2 at 70°C for 48 hours did not yield any observable CO_2 reduction product, even in the presence of PPh_3.[22] As such, a catalyst is required to lower the energy barrier and provide access to HCOOBcat (**IM1**, -11.0 *(+1.5)* kcal.mol^{-1}).

As was previously reported, the adduct between CO_2 and ambiphilic compound **1** (1-Bcat-2-PPh_2-C_6H_4) was never observed spectroscopically.[22] Theoretical results suggest that the adduct formation between **1** and CO_2 is endothermic by +6.8 kcal.mol^{-1} (**IM0**, +6.8 *(+20.8)* kcal.mol^{-1}). The binding of CO_2 induces a pyramidalization at the boron center, modifying the coordination environment of the catalyst. In fact, while the sum of the angles around the boron center in **1** is 359.9°, indicative of a sp^2 planar geometry, the sum of the same angles in **IM0** is 334.4°. Intermediate **IM0** counts four Lewis basic sites that can potentially bind catecholborane (HBcat). Indeed, coordination of the hydroborane to a nucleophilic site is required to promote the hydroboration of carbonyl-containing fragments.[37] In order to simplify the discussion, the Lewis basic sites were numbered 1 through 4 as illustrated in Scheme 2.

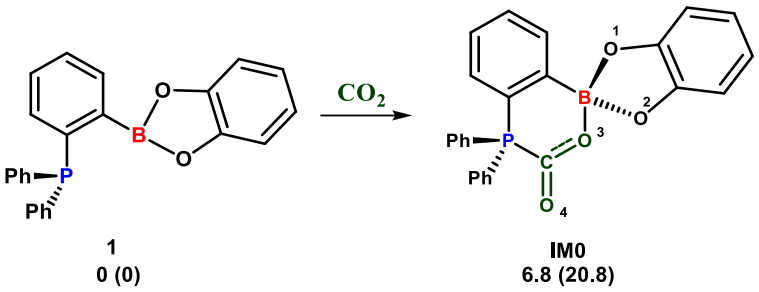

Scheme 2. Reaction of **1** with CO_2, generating **IM0** illustrating the potential binding sites for HBcat.

Firstly, no transition state (TS) could be located for the reduction of CO_2 via the coordination of HBcat to sites 1 and 3, mainly due to the geometric constraints that prevent the hydride transfer to the carbonyl moiety. Consequently, all four possible pathways (labeled **A** through **D**), involving coordination to the two remaining sites as well as direct coordination to the phosphorus atom of **1** were studied for the initial reduction step and are described below. The most direct reduction path (pathway A, Scheme 3) involves the coordination of HBcat to site 4, generating the classical 4-membered ring hydroboration transition state (**TS1A**) as suggested by Dimar for the reduction of a variety of aldehydes and ketones by hydroboration.[37] For such a process, the barrier was found to be relatively high, although accessible at +24.4 *(+55.7)* kcal.mol^{-1}, generating **IM1A** (-13.1 *(+16.0)* kcal.mol^{-1}).[38] Therefore, pathway A does not appropriately represent the reduction of CO_2 to HCOOBcat by catalyst **1**.

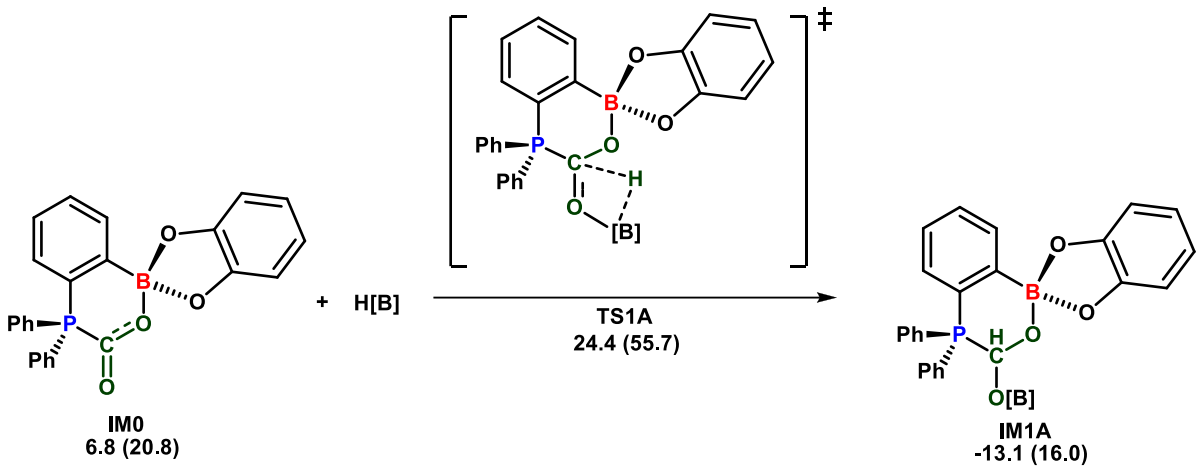

Scheme 3. Pathway A: hydroboration reaction of CO_2 through a classical 4-membered transition state. [B] = Bcat

Coordination of HBcat to site 2 generates intermediate **IM0B** (-2.1 *(+26.5)* kcal.mol^{-1}) which is only slightly thermodynamically stabilized with respect to **IM0** (Pathway B, Scheme 4). From the adduct **IM0B**, the hydride can be transferred to the carbon atom of CO_2 through a 6-membered ring transition state (**TS1B**, +16.7 *(+46.0)* kcal.mol^{-1}), yielding **IM1B** (-17.7 *(+12.2)* kcal.mol^{-1}). Such reactivity is reminiscent of the hydroboration mechanism observed with oxazaborozilidine catalysts developed by Corey *et al.* where the coordination of the borane to a Lewis base promotes intramolecular hydride delivery.[39] It should be noted that pathway B is kinetically more accessible than pathway A since the TS is 7.7 kcal.mol^{-1} lower in energy.

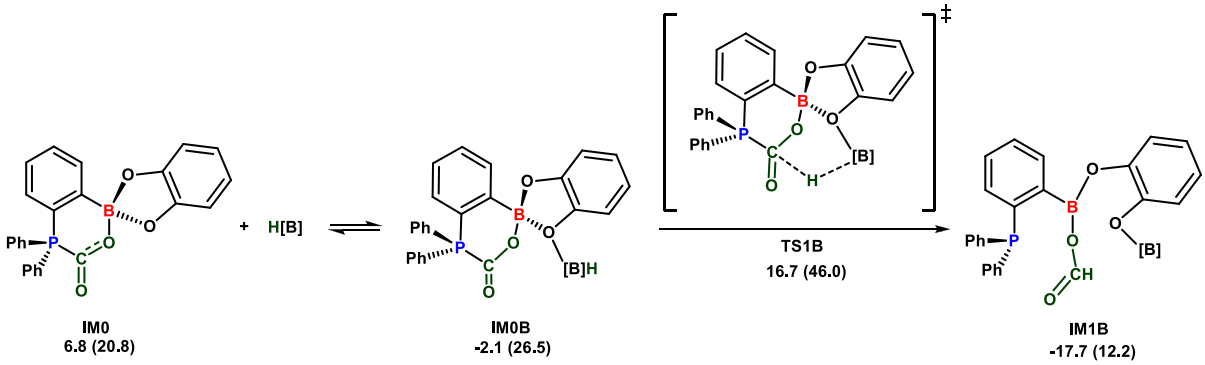

Scheme 4. Pathway B: hydroboration through coordination of HBcat to the catechol fragment followed by intramolecular hydride delivery. [B] = Bcat

A third pathway can be considered in which both the reducing agent and CO_2 are simultaneously activated. The phosphorus atom activates catecholborane while CO_2 is activated by the boron fragment. The coordination of the Lewis base increases the electronic density at the boron center, therefore making the hydride more nucleophilic. In fact, the hydride activation of catecholborane by a variety of phosphines, including triphenylphosphine, has been reported in the past and was shown to occur readily at room temperature.[40] Hence, pathway C (Scheme 5), involving **TS1C**, (+10.8 *(+38.3)* kcal.mol^{-1}) and leading to **IM1C** (-17.8 *(+12.0)* kcal.mol^{-1}), is even more energetically favorable than pathways A and B. The simultaneous activation of the reducing agent and the substrate drastically contrasts from the classical view of CO_2 activation by FLP systems where the emphasis is on the sole activation of carbon dioxide by both functionalities. Very bulky groups on the catalyst framework, notably on the Lewis base, may restrict the interaction with the hydride source, decreasing the reactivity of the system.

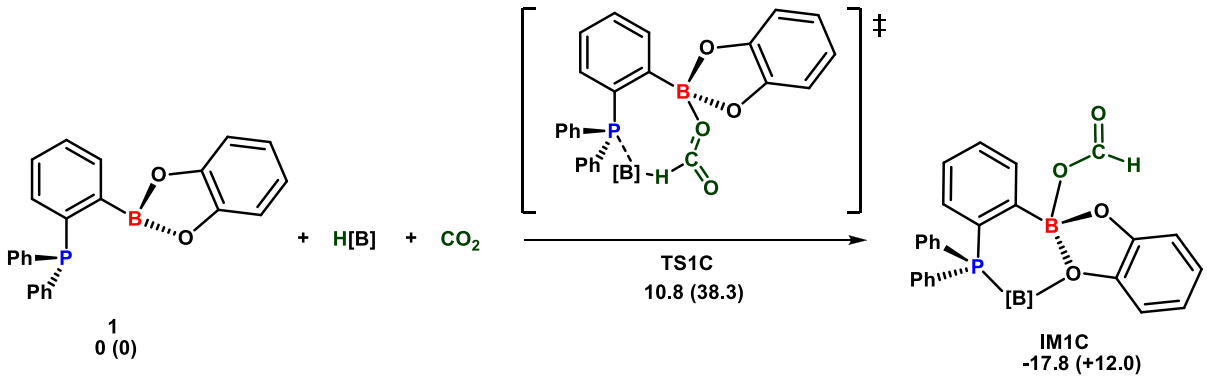

Scheme 5. Pathway C: hydroboration through simultaneous Lewis base activation of the borane and Lewis acid activation of CO_2. [B] = Bcat

Consistently with the experimental results where no reaction was observed when heating catecholborane in the presence of **1**,[22] no minimum was found on the potential energy surface for the formation of an adduct between HBcat and the catalyst. However, further theoretical investigation shows possible rearrangements leading to other plausible intermediates. Indeed, as represented in Scheme 6, HBcat can add to one of the B-O bonds of the catalyst through **TS0D** (+19.0 *(+35.7)* kcal.mol^{-1}) to generate intermediate **IM0D** (-0.2 *(+18.4)* kcal.mol^{-1}), that upon addition of CO_2, generates intermediate **IM0D'** (+4.7 *(+34.4)* kcal.mol^{-1}). The latter can be described as a hydridoborate/boronium bifunctional system where the binding of CO_2 is ensured by the assistance of the catecholboronium fragment which makes CO_2 more prone to nucleophilic attacks. At the same time, the phosphine moiety acts as an anchor point, allowing the fixation of CO_2 with an ideal orientation for hydride delivery from the hydridoborate fragment. The hydride delivery occurs at **TS1D** (+12.5 *(+43.3)* kcal.mol^{-1}), leading to the regeneration of the catalyst by release of HCOOBcat. This completes an alternate reaction path for the initial step of CO_2 reduction (pathway D, Scheme 6). Such reactivity is somewhat reminiscent of the catalytic reduction of imines by boronium hydridoborate ion pairs reported by Crudden *et al.* [41]

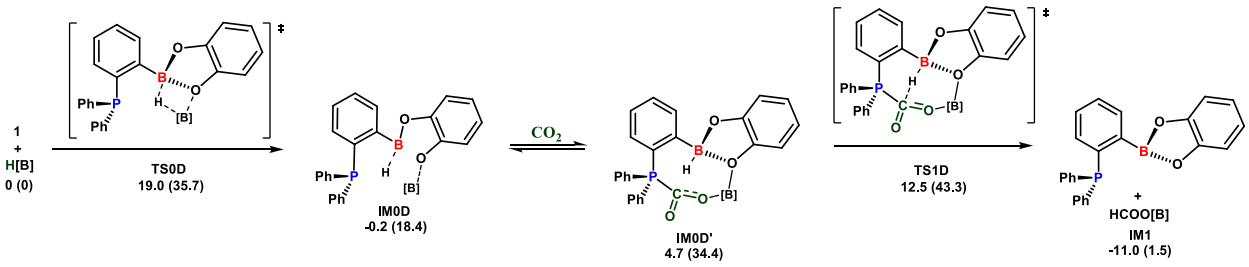

Scheme 6. Pathway D: CO_2 reduction through the generation of a boronium / hydridoborate ion pair. [B] = Bcat

Summing up the results for the reduction of CO_2 to HCOOBcat (Figure 1), the direct hydroboration through pathway A can be ruled out. Although the activation of HBcat by one of the oxygen atoms of **1** (pathway B) or through hydride transfer from HBcat to the catalyst (pathway D) are plausible, pathway C is the most easily accessible and yields **IM1C** with a net energetic gain of 17.8 kcal.mol^{-1}. The catalyzed reduction leads to a decrease of the activation energy by 23.4 kcal.mol^{-1} when compared to the uncatalyzed system, making the reduction kinetically manageable.

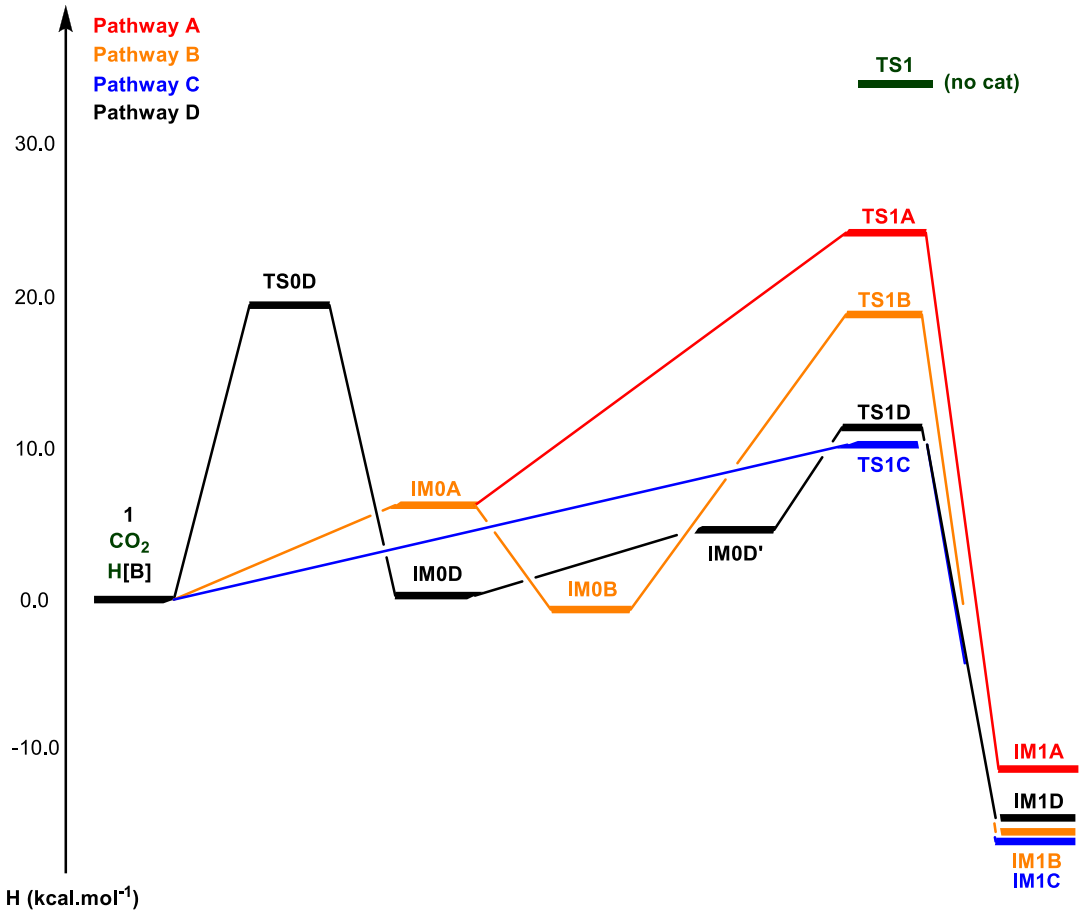

Figure 1. Important intermediates and transition states for the catalyzed reduction of CO_2 to HCOOBcat.

Second reduction step: from HCOOBcat to CH_2O and derivatives

Before determining the possible role of the catalyst in the second reduction step, the uncatalyzed hydroboration of HCOOBcat was investigated thoroughly. From HCOOBcat (**IM1**), the reduction occurs through a classical four-membered ring transition state, **TS2** +15.8 (+45.0) or **TS2'** (+14.1 *(+42.7)* kcal.mol^{-1}), yielding catBOCH$_2$OBcat (**IM2**, -40.6 *(-11.6)* kcal.mol^{-1} or formaldehyde (**IM2'** -30.8 *(-15.6)* kcal.mol^{-1}), respectively (See ESI). (Scheme 7)

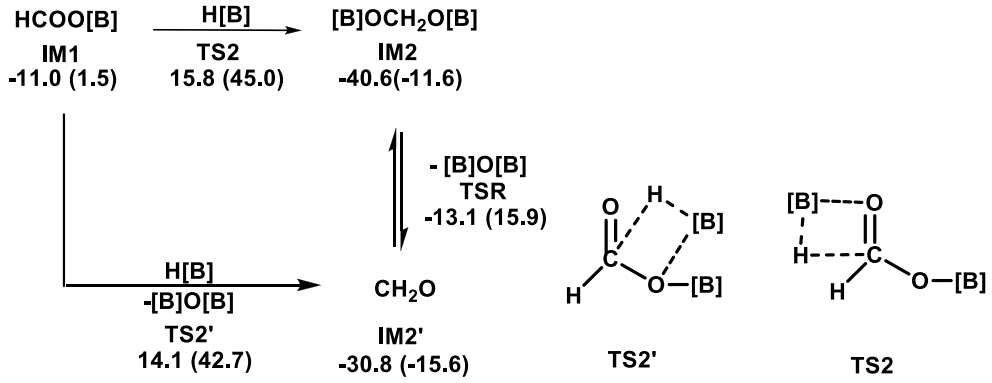

Scheme 7. Catalyst free reduction of HCOOBcat to catBOCH$_2$OBcat or formaldehyde. [B]=Bcat

The transition state **TS2** has been previously reported in the work of Wang *et al.*, but the authors have concluded that the energy barrier was too high for the reactions to occur at room temperature.[Erreur ! Signet non défini.b] On the other hand, it has been reported that the reaction of catecholborane with carboxylic acids of the type RCOOH (R=alkyl) at room temperature yields the corresponding acyloxyboranes (RCOOBcat) as intermediates as well as H_2.[42] The addition of two supplementary equivalents of HBcat results in the formation of RCH$_2$OBcat, leading to the corresponding alcohol after aqueous work-up. In order to verify that the reduction of HCOOBcat

by HBcat was indeed possible, the reaction between HBcat and formic acid (HCOOH) was studied experimentally.

The addition of formic acid (1 equiv) to a slight excess of catecholborane (3.3 equiv) at room temperature led to the rapid evolution of dihydrogen. As expected, monitoring of the reaction using ^{1}H NMR spectroscopy revealed the presence of HCOOBcat as an intermediate species, but after 90 minutes, the signals attributed to HCOOH and HBcat disappeared completely, resulting in total conversion to CH_3OBcat and catBOBcat. The nature of the products was confirmed by $^{11}B\{^{1}H\}$ NMR spectroscopy and confirmed based on literature precedents. [22]

Repeating the same experiment at 70°C yielded complete conversion after only 15 minutes. With a computed barrier of +25.1 *(+41.2)* kcal.mol^{-1} for the hydroboration of HCOOBcat by HBcat, it is clear that the reaction occurs much faster than what was previously assumed from computational results and that HCOOBcat can be reduced without the implication of a catalyst. (Scheme 8)

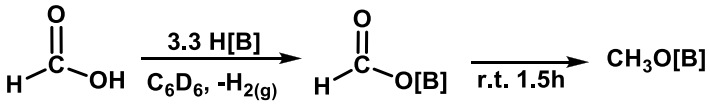

Scheme 8. Experimental verification for the hydroboration of formic acid by catecholborane. [B]=Bcat

However, in contrast to the other reported systems for the catalytic hydroboration of carbon dioxide where formatoborate species were observed during catalysis, [7,23,**Erreur ! Signet non défini.**] no trace of HCOOBcat was observed during catalysis.[21] Indeed, no HCOOBcat could be detected even when monitoring at room temperature the reaction between 1 equiv of HBcat relative to catalyst **1** under 1 atm of CO_2. The only new species that was observed in this reaction mixture

was the formaldehyde adduct **2** (Scheme 9). This result suggests that contrarily to all reported systems where the catalysts are of importance in the first reduction step, catalyst **1** is playing an important role in the reduction of the formatoborate species. Such result is in line with the previously reported results showing that **1** catalyzed the hydroboration of methylformate.[22]

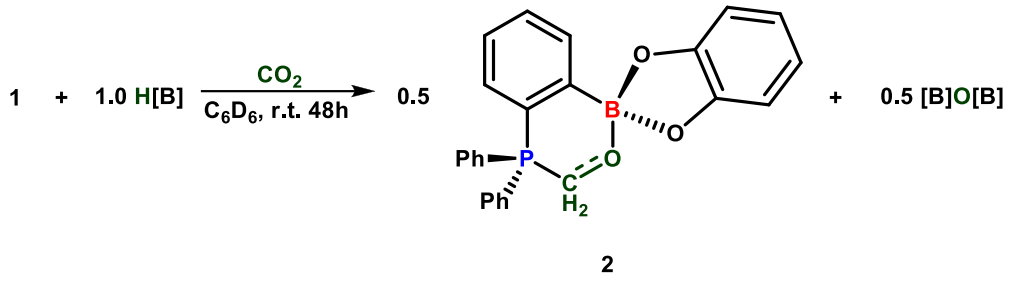

2

Scheme 9. Attempt to isolate HCOOBcat, leading to the exclusive formation of **2** (**IM2C'**). [B]= Bcat

In order to reveal how this reduction step is catalyzed, the interaction of HCOOBcat (**IM1**) with catalyst **1** was studied computationally. The most favored interaction (**IM1C**, -17.8 *(+12.0)* kcal.mol^{-1}) being slightly exothermic by -6.8 kcal.mol^{-1} with respect to the free reagents suggests that some of the HCOOBcat molecules will remain bound to the catalyst. However, each isomer observed in Scheme 10 can still be considered as a potential intermediate for the subsequent hydroboration reaction and as such, one must also take into account the possible rearrangements of **IM1C**.

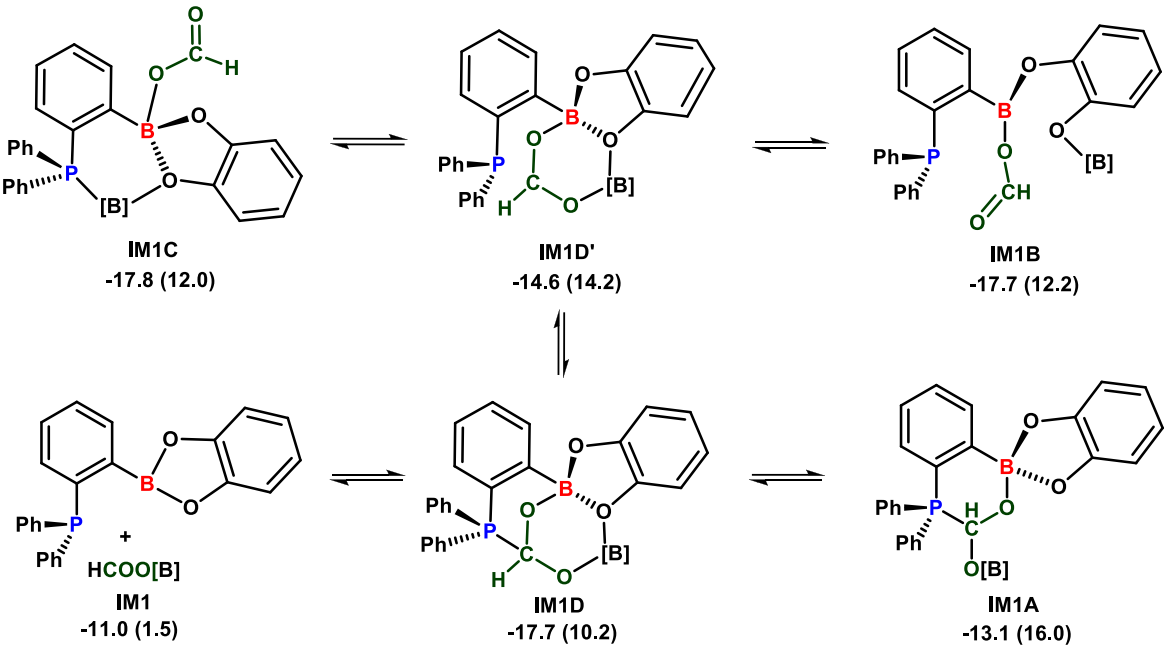

Scheme 10. Possible interactions and rearrangements of HCOOBcat with catalyst **1**. [B]=Bcat

Interestingly, no suitable transition state was found directly from **IM1D**. This is in line with the study of Musgrave *et al.* where it was demonstrated that even if the binding of a phosphine center to CO_2 was beneficial for the fixation of the CO_2 molecule on a catalyst, a strong P-C interaction may actually hinder hydride transfer since the electrophilic site on carbon is occupied by the free electron pair of phosphorus.[43] An interesting situation occurs in the case of **IM1D'**, where the phosphine is no longer interacting with the electrophilic carbon atom of the activated substrate. The activation of a HBcat molecule by the phosphorus moiety, as previously observed for pathway C, leads to hydride transfer through the most accessible TS for the reduction of HCOOBcat, **TS2C** (-13.6 *(+32.2)* kcal.mol^{-1}), generating **IM2C** (-48.0 *(-2.2)* kcal.mol^{-1}) with a net energetic gain of 34.4 kcal.mol^{-1} (Scheme 11).

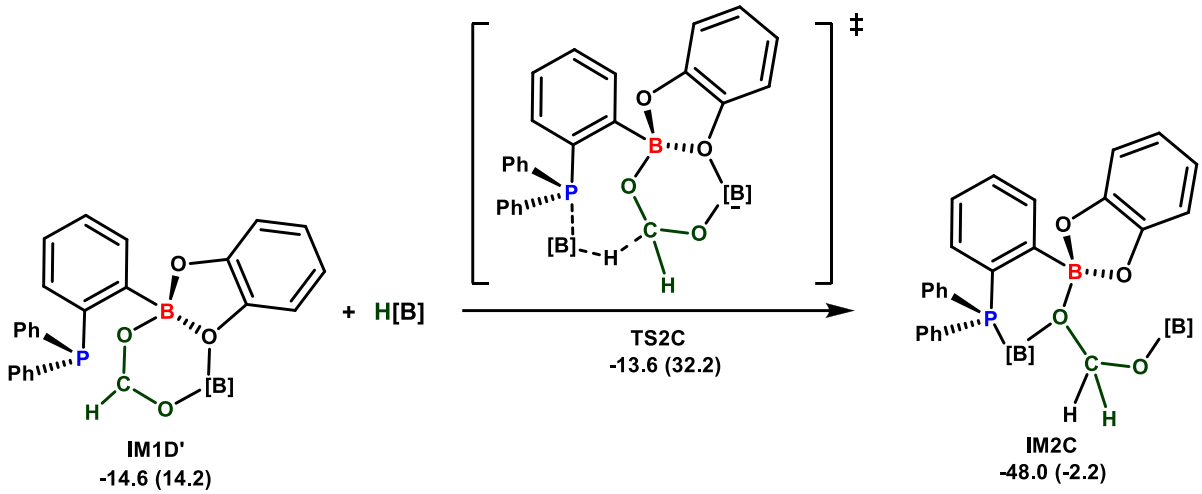

Scheme 11. Suggested pathway for the catalyzed reduction of HCOO[B] involving the catalyst [B]=Bcat

Other pathways are also less favored as the hydroboration through four-membered ring transition states similar to pathway A, either from **IM1B** or **IM1C,** and leading to catBOCH$_2$OBcat type reduction products were found unlikely (see ESI). Alternately, hydride transfer through coordination of HBcat to the catechol oxygen atom of **IM1D**, similar to what was observed in pathway B (Scheme 4) and leading to formaldehyde and catBOBcat, although accessible, proved to be less favored than **TS2C** (see ESI). These results underline the beneficial effect of double Lewis acid activation while reinforcing the concept of hydride activation by the Lewis basic center since the catalyzed reduction is 20.9 kcal.mol^{-1} more favored than the catalyst free reduction. (Figure 2)

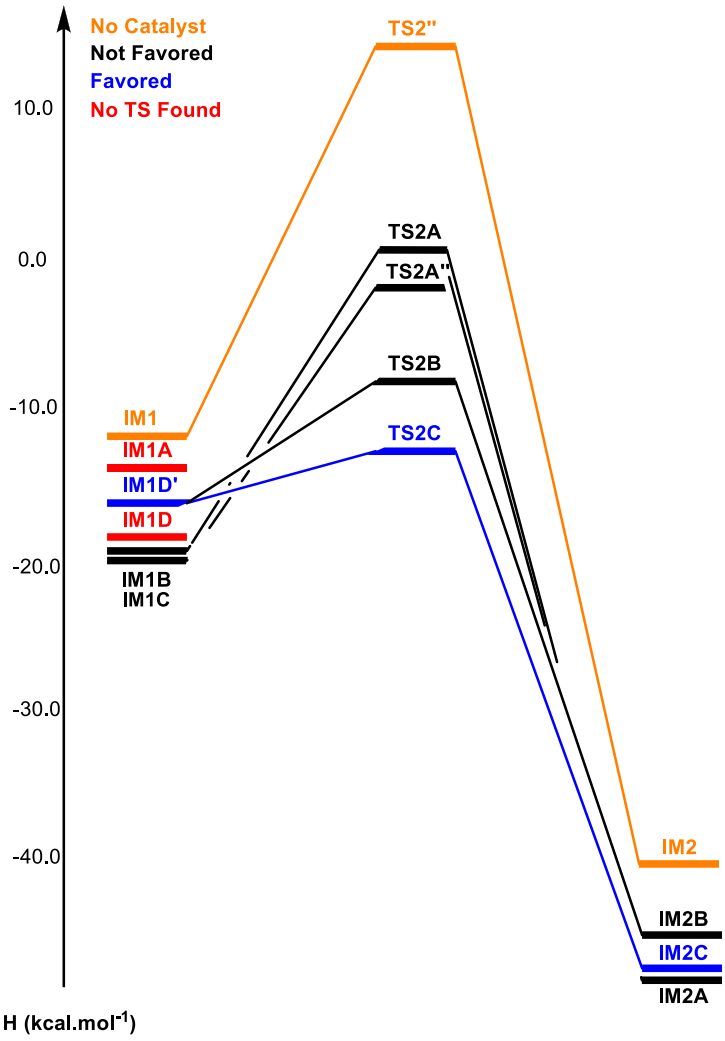

Figure 2. Relative energies of transition states and intermediates for the reduction of HCOOBcat to CH_2O or cat$BOCH_2OB$cat.

Third reduction step: reducing CH_2O and derivatives to CH_3OBcat

Although species **2** was previously characterized in solution, it was possible to observe in the reduction process at 25 °C the formation of a crystalline solid that was identified as the formaldehyde adduct, thus confirming the presence of this intermediate (Figure 3). The various

bond lengths in the crystal structure of **2** are in accordance to the computational data, thus once more confirming the validity of the method.

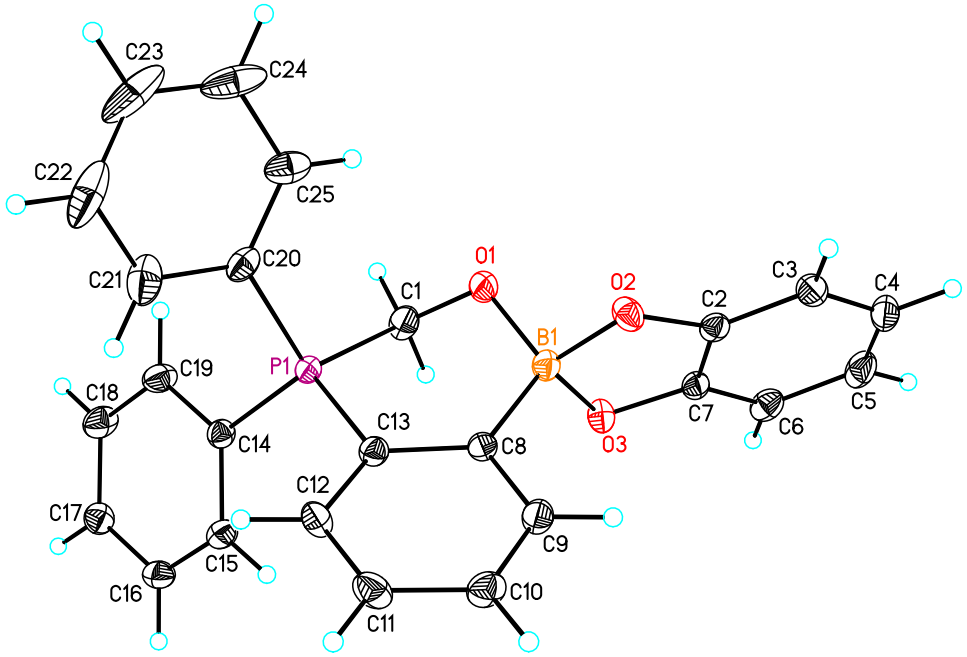

Figure 3. ORTEP drawing of **2** with the anisotropic atomic displacement ellipsoids shown at 50% probability level. Selected bond lengths [Å] and angles [°]: P(1)-C(1) 1.823(2), C(1)-O(1) 1.402(3), O(1)-B(1) 1.473(3), C(13)-P(1)-C(1) 104.74(9), C(8)-C(13)-P(1) 117.28(14), C(13)-C(8)-B(1) 125.32(16), C(1)-O(1)-B(1)113.67(15).

Therefore, **IM2C** must rearrange to this more stable intermediate. Having a closer look at **IM2C**, it is better described as a simple adduct between **1** and catBOCH$_2$OBcat where the interactions occur through dative P-B and B-O bonds. However, the binding is favored by only -7.4 *(+9.4)* kcal.mol^{-1}. As can be observed in Scheme 12, catBOCH$_2$OBcat may rearrange to generate CH$_2$O by releasing catBOBcat (**IM2'** -30.8 *(-15.6)* kcal.mol^{-1}). Such a rearrangement was also assumed

to happen by Wang *et al.* in their related theoretical study of a catalytic CO_2 hydroboration system.[Erreur ! Signet non défini.b] The system is then stabilized by the trapping of formaldehyde by **1** to generate **IM2C' (2).** The entropic stabilization due to the release of a catBOBcat molecule is thought to be the driving force for the formation of this intermediate.

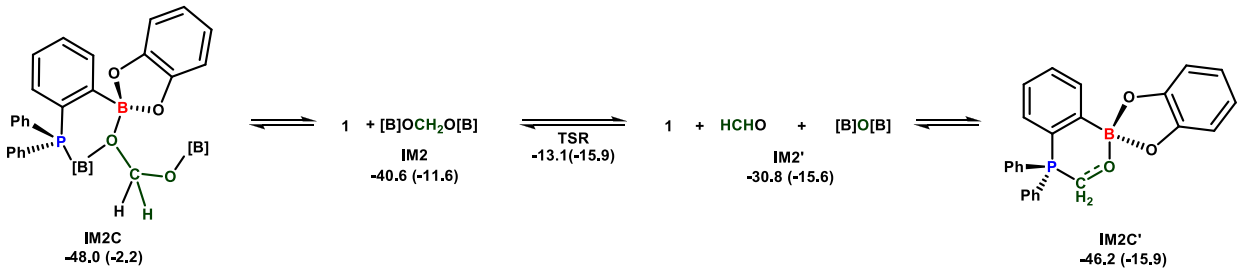

Scheme 12. Formation of **IM2C' (2)** through the rearrangement of catBOCH$_2$OBcat to CH$_2$O. [B]=Bcat

It is widely known that aldehydes are readily reduced by hydroboranes, but we were curious to see if the trapping of formaldehyde by catalyst **1** would hinder or favor the reduction. Since formaldehyde readily polymerizes to paraformaldehyde and the solubility of **2** in common NMR solvents is very limited, 4-bromobenzaldehyde **3** was chosen as a model compound. Monitoring of the reaction between **3** and 1.1 equiv of HBcat showed that the reduction takes 90 minutes to yield complete conversion to the corresponding alkoxyborane **4**. Interestingly, repeating the reaction in identical conditions but in the presence of 2 mol % of **1** led to the complete conversion in less than 5 minutes, showing that **1** acts as a catalyst for the reduction of aldehydes to alkoxyboranes.(Scheme 13).

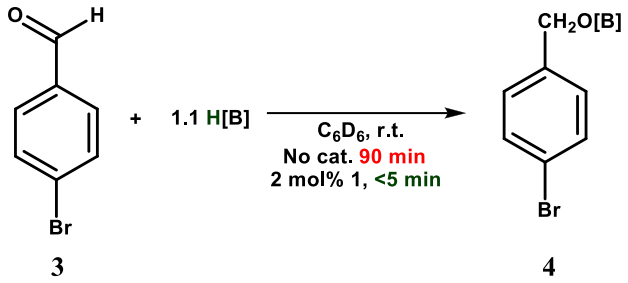

Scheme 13. Experimental verification for the catalytic role of **1** in the hydroboration of 4-bromobenzaldehyde by catecholborane. [B]=Bcat

This interesting result prompted us to investigate this final step computationally. From the formaldehyde adduct **IM2C'** (**2**), the activation of HBcat by the phosphine moiety (similar to pathway C) leads to **TS3C** (-36.2 *(7.3)* kcal.mol^{-1}), yielding the intermediate **IM3C** (-83.9 *(-38.5)* kcal.mol^{-1}). Note that **IM3C** can easily rearrange to **IM3** through **TS3D** (-72.6 *(-25.0)* kcal.mol^{-1}), regenerating catalyst **1** and producing CH_3OBcat (Scheme 14).

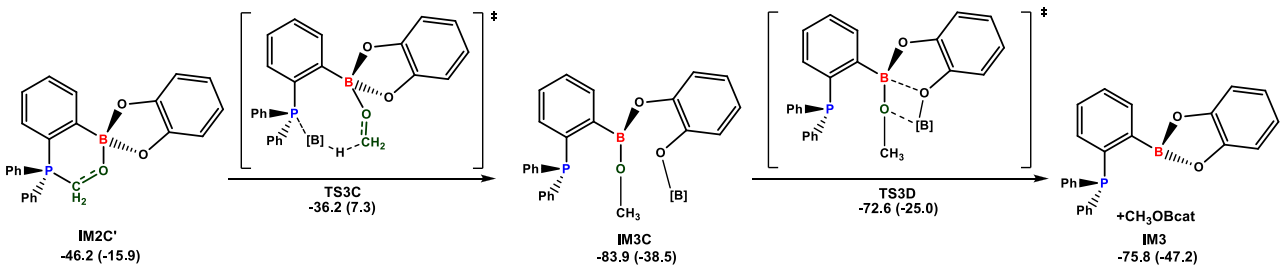

Scheme 14. Catalyzed reduction of formaldehyde to CH_3OBcat, regenerating the catalyst. [B]=Bcat

The final reduction step represents an energetic gain of 25.8 kcal.mol^{-1}. The catalyzed reduction is 10.2 kcal.mol^{-1} more favored than the catalyst free reduction. All other pathways (similar to pathways A or B) are less favorable (See ESI). (Figure 4)

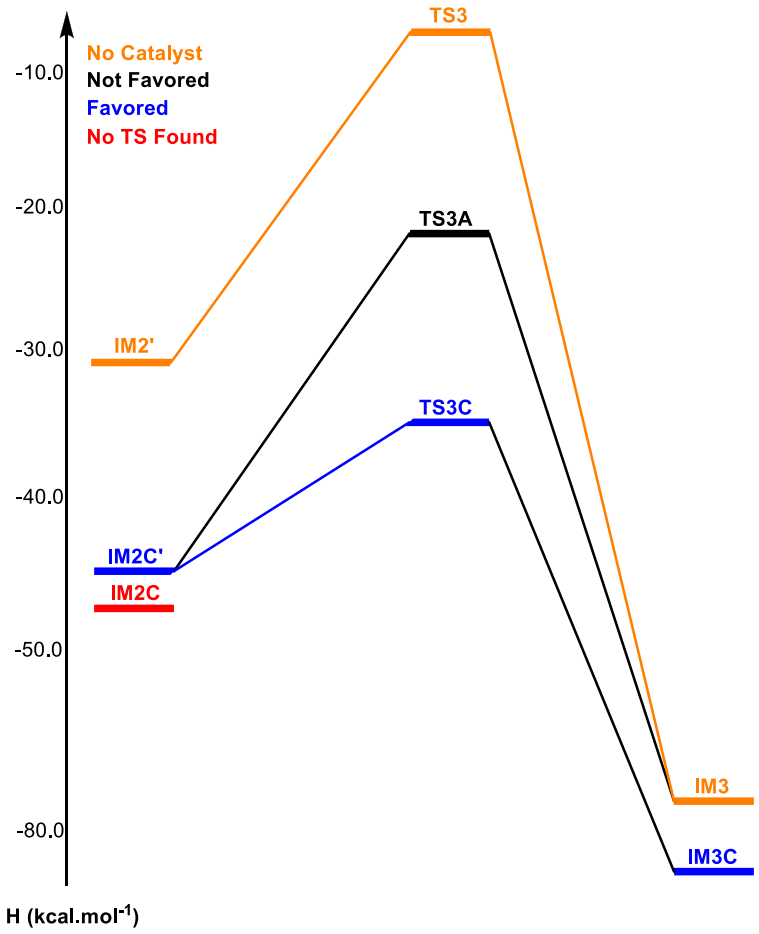

Figure 4. Relative energies of transition states and intermediates for the reduction of CH_2O to CH_3OBcat.

Discussion

As discussed above, the catalyst is essential to lower the energy gap for the reduction of CO_2 to HCOOBcat to occur, but also plays a significant role in enhancing the rates of the subsequent

reduction steps. The most favorable species for the reduction in the first step is the possibility of having the Lewis acidic site of the catalyst binding CO_2 while the phosphine activates the borane to deliver a hydride to the activated electrophilic carbon of carbon dioxide. Together, these factors lead to a lowering of 23.4 kcal.mol^{-1} of the energy barrier when compared to the catalyst free reduction. This pathway puts emphasis on the fact that the role of the catalyst is to simultaneously activate both of the reagents and not CO_2 alone.

The reduction of both HCOOBcat and CH_2O was shown to be possible without any implication from the catalyst and consequently, some of these reductions are expected to occur catalyst-free in the presence of a large excess of HBcat. However, activation of the HBcat moiety by the phosphorus center while the substrate is fixed and activated by the Lewis acidic boron center results in lowering the transition state energies by 20.9 and 10.2 kcal.mol^{-1} for the hydroboration of HCOOBcat and CH_2O respectively. The rapid reduction of HCOOBcat by the catalyst and in the reaction medium explains why it could not be observed experimentally. On the other hand, the 15.4 kcal.mol^{-1} bonding interaction of the catalyst with formaldehyde rationalizes the fact that this particular adduct can be observed by NMR spectroscopy during catalysis. As it was found out in this study, **2** even crystallizes out of the reaction medium at ambient temperature, while everything is soluble at 70 °C. This aspect might explain the lower activity of this system at room temperature and the high enhancement of the catalytic turn-overs with a relatively slight increase in temperature. The entire catalytic process is summarized in Scheme 15.

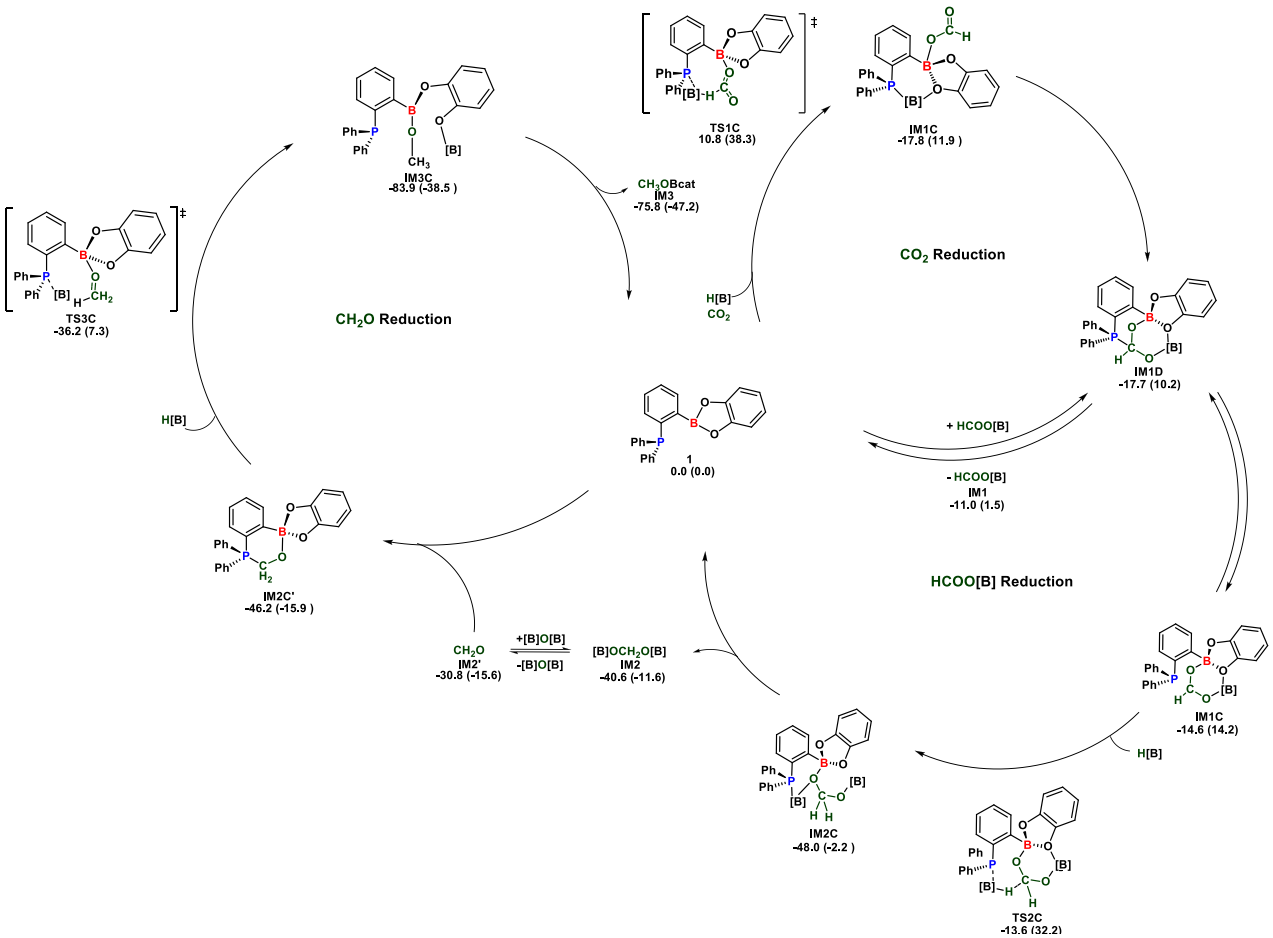

Scheme 15. Proposed mechanistic pathway including important transition states for the reduction of CO_2 to CH_3OBcat by **1**. [B]=Bcat.

Taking these results into account, the classical FLP approach of using very bulky substituents may lead to a more difficult activation of substrates. While a strongly Lewis basic phosphine might bind CO_2 and other intermediates more strongly and hinder hydride transfer, it may also activate the reductant more effectively and increase catalytic activity. However, the use of a moderate Lewis acid allows the release of the various hydroboration products in the reaction medium, allowing their liberation from the catalyst. A key aspect of the system is the presence of

both the Lewis acid and base in a single molecule, reducing the entropic cost of every catalyzed step. Finally, the importance of the oxygen substituents on the boron center cannot be overlooked as their dynamic nature allows the formation of a number of isomers and intermediates for a very flexible catalyst.

Conclusion

In conclusion, the full mechanism for the first catalytic hydroboration of carbon dioxide by a FLP based system **1** was determined. The catalyst was shown to catalyze every step of the reaction. The findings reported herein offer important insight on the aspects that need to be considered for the design of ambiphilic catalysts. Current work focuses on preparing new ambiphilic catalysts by varying the functional groups on phosphorus and boron in order to achieve maximal catalytic efficiency and broaden the scope of reducing agent to hydrosilanes. We are hopeful that these findings will inspire unprecedented FLP chemistry and novel catalytic applications.

Supporting Information

Detailed experimental procedures and additional DFT information (other calculated reaction pathways, cartesian coordinates, free enthalpies and energies). This material is available free of charge via the Internet at http://pubs.acs.org.

AUTHOR INFORMATION

Corresponding Author

E-mail: frederic.fontaine@chm.ulaval.ca; laurent.maron@irsamc.ups-tlse.fr

Notes

The authors declare no competing financial interests.

ACKNOWLEDGMENTS

This work was supported by the National Sciences and Engineering Research Council of Canada (NSERC, Canada) and the Centre de Catalyse et Chimie Verte (Quebec). M.-A. C. and M.-A. L. would like to thank NSERC and FQRNT for scholarships. We would like to acknowledge R. Nadeau for the TOC graphic. We acknowledge W. Bi for the resolution of the crystal structure. We acknowledge D. Bourissou for insightful discussions. LM is member of the Institut Universitaire de France. Cines and CALMIP are acknowledged for a generous grant of computing time. The Humboldt foundation is also acknowledged for financial support.

References

[1] Olah, G. A.; Goeppert, A.; Surya Prakash, G. K. *J. Org. Chem.* **2009**, *74*, 487-498.

[2] D'Alessandro, D. M.; Smit, B.; Long, J. R. *Angew. Chem. Int. Ed.* **2010**, *49*, 6058-6082.

[3] *Beyond Oil and Gas: The Methanol Economy* , George A. Olah, Alain Goeppert, G. K. Surya Prakash, Wiley-VCH, **2006.**

[4] (a) Tanaka, R.; Yamashita, M.; Nozaki, K.; *J. Am. Chem. Soc.* **2009**, *131*, 14168 – 14169. (b) Federsel, C.; Jackstell, R.; Beller, M. *Angew. Chem. Int. Ed.* **2010**, *49*, 6254 – 6257. (c) Schaub, T.; Paciello, R. A. *Angew. Chem. Int. Ed.* **2011**, *50*, 7278 – 7282

[5] (a) Matsuo, T.; Kawaguchi, H. *J. Am. Chem. Soc.* **2006**, *128*, 12362 – 12363. (b) Park, S.; Bézier, D.; Brookhart, M. *J. Am. Chem. Soc.* **2012***, 134*, 11404 –11407 (c) Mitton, S. J.; Turculet, L. *Chem. Eur. J.* **2012**, *48*, 15258-15262. (d) Langer, R.; Diskin-Posner, Y.; Leitus, G. W.; Shimon, L. J.; Ben-David, Y.; Milstein, D. *Angew. Chem. Int. Ed.* **2011**, *50*, 9948 – 9952. (e) Federsel, C.; Boddien, A.; Jackstell, R.; Jennerjahn, R.; Dyson, P. J.; Scopelliti, R.; Laurenczy, G.; Beller, M. *Angew. Chem. Int. Ed.* **2010**, *49*, 9777 – 9780. (f) Huff, C. A.; Sanford, M. S. *ACS Catal.* **2013**, *3*, 2412-2416. (g) Jeletic, M. S.; Mock, M. T.; Appel, A. M.; Linehan, J. C. *J. Am. Chem. Soc.* **2013**, *135*, 11533−11536. (h) Zhang, L.; Cheng, J.; Hou, Z. *Chem. Commun.* **2013**, *49*, 4782−4784.

[6] Bontemps, S.; Sabo-Etienne, S. *Angew. Chem., Int. Ed*. **2013**, *52*, 10253-10255 (b) Bontemps, S.; Vendier, L.; Sabo-Etienne, S. *J. Am. Chem. Soc.* **2014**, *136*, 4419−4425

[7] (a) Chakraborty, S.; Zhang, J.; Krause, J. A.; Guan, H. *J. Am. Chem. Soc.* **2010**, *132*, 8872-8873. (b) Balaraman, E.; Gunanathan, C.; Zhang, J.; Shimon, L. J. W.; Milstein, D. *Nat. Chem.* **2011**, *3*, 609 –614. (c) Huff, C. A.; Sanford, M. S. *J. Am. Chem. Soc.* **2011,** *133*, 18122-18125.

(d) Wesselbaum, S.; von Stein, T.; Klankermayer, J.; Leitner, W. *Angew. Chem., Int. Ed.* **2012,** *51*, 7499 –7502.

[8] (a) Matsuo, T.; Kawaguchi, H. *J. Am. Chem. Soc.* **2006**, *128*, 12362 – 12363. (b) Park, S.; Bézier, D.; Brookhart, M. *J. Am. Chem. Soc.* **2012**, *134*, 11404 –11407. (c) Mitton, S. J.; Turculet, L. *Chem. Eur. J.* **2012**, *48*, 15258-15262. (d) Berkefeld, A.; Piers, W. E.; Parvez, M.; Castro, L.; Maron, L.; Eisenstein, O. *Chem. Sci.* **2013**, *4*, 2152-2162.

[9] LeBlanc, F. A.; Piers, W. E.; Parvez, M. *Angew. Chem. Int. Ed.* **2014**, *126*, 808 –811.

[10] (a) Zhang, L.; Cheng, J.; Hou, Z. *Chem. Commun.*, **2013**, *49*, 4782–4784.

[11] (a) Khandelwal, M.; Wehmschulte, R. J. *Angew. Chem. Int. Ed.* **2012**, *51*, 7323–7326.

(b) Wehmschulte, R. J.; Saleh, M.; Powell, D. R. *Organometallics*, **2013**, *32*, 6812–6819.

[12] Schäfer, A.; Saak, W.; Haase, D.; Müller, T. *Angew. Chem. Int. Ed.* **2012**, *51*, 2981 –2984.

[13] (a) Mömming, C.; Otten, M.; Kehr, E. G.; Fröhlich, R.; Grimme, S.; Stephan, D. W.; Erker, G. *Angew. Chem. Int. Ed.* **2009**, *48*, 6643 – 6646. (b) Appelt, C.; Westenberg, H.; Bertini, F.; Ehlers, A. W.; Slootweg, J. C.; Lammertsma, K.; Uhl, W. *Angew. Chem. Int. Ed.* **2011**, *50*, 3925-3928.

(c) Boudreau, J., Courtemanche, M-A.; Fontaine, F-G. *Chem. Commun.* **2011**, *47*, 11131-11133**.**

(d) Peuser, I.; Neu, R. C.; Zhao, X.; Ulrich, M.; Schirmer, B.; Tannert, J. A.; Kehr, G.; Fröhlich, R.; Grimme, S.; Erker, G.; Stephan, D. W. *Chem. Eur. J.* **2011**, *17*, 9640-9650. (e) Hounjet, L. J.; Caputo, C. B.; Stephan, D. W. *Angew. Chem. Int. Ed.* **2012**, *51*, 4714 – 4717. (f) Takeuchi, K.; Stephan, D. W. *Chem. Commun.* **2012,** *48*, 11304-11306. (g) Theuergarten, E.; Schlösser, J.; Schlüns, D.; Freytag, M.; Daniliuc, C. G.; Jones, P. G.; Tamm, M. *Dalton Trans.* **2012,** *41*, 9101-9110. (h) Lu, Z.; Y. J, Liu.; Wang, Y.; Lin, J.; Li, Z. H.; Wang, H. *Organometallics*, **2013**, *32* , 6753-6758. (i) Barry, B. M.; Dickie, D. A.; Murphy, L. J.; Clyburne, J. A. C.; Kemp, R. A. *Inorg. Chem.* **2013,** *52*, 8312-8314.

[14] Dobrovetsky, R.; Stephan, D. W. *Angew. Chem., Int. Ed.* **2013**, *52*, 2516−2519.

[15] (a) Ménard, G.; Stephan, D. W. *J. Am. Chem. Soc.* **2010**, *132*, 1796–1797. (b) Ashley, A. E.; Thompson. A. L.; O'Hare, D. *Angew. Chem., Int. Ed.* **2009**, *48*, 9839–9843. (c) Ménard, G.; Stephan, D. W. *J. Am. Chem. Soc.* **2010**, *132*, 1796 –1797. (d) Ménard, G.; Stephan, D. W. *Dalton Trans.* **2013**, *42*, 5447 – 5453. (e) Roy, L.; Zimmerman, P. M.; Paul, A. *Chem. Eur. J.* **2011**, *17*, 435 –439. (f) Ménard, G.; Gilbert, T. M.; Hatnean, J. A.; Kraft, A.; Krossing, I.; Stephan, D. W. *Organometallics*, **2013**, *32*, 4416 – 4422.

[16] (a) Berkefeld, A.; Piers, W. E.; Parvez, M. *J. Am. Chem. Soc.* **2010**, *132*, 10660 – 10661. (b) Wen, M.; Huang, F.; Lu, G.; Wang, Z.-X. *Inorg. Chem.* **2013**, *52*, 12098 –12107.

[17] Riduan, S. N., Zhang, Y. ; Ying, J. Y. *Angew. Chem., Int. Ed.* **2009**, *48*, 3322-3325.

[18] (a) Das Neves Gomes, C.; Jacquet, O; Villiers, C.; Thuéry, P, Ephritikhine, M.; Cantat, T. *Angew. Chem., Int. Ed.* **2012**, *51*, 187-190. (b) Jacquet, O; Gomes, C. D.; Ephritikhine, M.; Cantat, T. *J. Am. Chem. Soc.* **2012**, *134*, 2934-2937.

[19] Das Neves Gomes, C.; Blondiaux, E.; Thuéry, P.; Cantat, T. *Chem. Eur. J.* **2014**, *23*, 7098-7106.

[20] Wang, T.; Stephan, D. W. *Chem. Commun.* **2014,** Advance article, DOI: 10.1039/C4CC02103G.

[21] Courtemanche, M.-A.; Larouche, J.; Légaré, M.-A.; Wenhua, B.; Maron, L.; Fontaine, F.-G. *Organometallics*, **2013**, *32*, 6804– 6811.

[22] (a) Courtemanche, M.-A.; Légaré, M.-A.; Maron, L.; Fontaine, F.-G. *J. Am. Chem. Soc.* **2013**, *135*, 9326-9329. (b) Fontaine, F.-G.; Courtemanche, M.-A.; Légaré, M.-A. *Chem. Eur. J.* **2014**, *20*, 2990-2996.

[23] Wang, T.; Stephan, D. W. *Chem. Eur. J.* **2014**, *20*, 3036-3039.

[24] Frisch, M. J.; Trucks, G. W.; Schlegel, H. G.; Scuseria, G. E.; Robb, M. A.; Montgomery, J. A., Jr.; Vreven, T.; Kudin, K. N.; Burant, J. C.; Millam, J. M.; Iyengar, S. S.; Tomasi, J.; Barone, V.; Mennucci, B.; Cossi, M.; Scalmani, G.; Rega, N.; Petersson, G. A.; Nakatsuji, H.; Hada, M.; Ehara, M.; Toyota, K.; Fukuda, R.; Hasegawa, J.; Ishida, M.; Nakajima, T.; Honda, Y.; Kitao, O.; Nakai, H.; Klene, M.; Li, X.; Knox, J. E.; Hratchian, H. P.; Cross, J. B.; Bakken, V.; Adamo, C.; Jaramillo, J.; Gomperts, R.; Stratmann, R. E.; Yazyev, O.; Austin, A. J.; Cammi, R.; Pomelli, C.; Ochterski, J. W.; Ayala, P. Y.; Morokuma, K.; Voth, G. A.; Salvador, P.; Dannenberg, J. J.; Zakrzewski, V. G.; Dapprich, S.; Daniels, A. D.; Strain, M. C.; Farkas, O.; Malick, D. K.; Rabuck, A. D.; Raghavachari, K.; Foresman, J. B.; Ortiz, J. V.; Cui, Q.; Baboul, A. G.; Clifford, S.; Cioslowski, J.; Stefanov, B. B.; Liu, A. L. G.; Piskorz, P.; Komaromi, I.; Martin, R. L.; Fox, D. J.; Keith, T.; Al-Laham, M. A.; Peng, C.; Nanayakkara, A.; Challacombe, M.; Gill, P. M. W.; Johnson, B.; Chen, W.; Wong, M.; Gonzalez, C.; Pople, J. A. Gaussian 03, Revision D.01; Gaussian, Inc.: Wallingford, CT, 2004.

[25] (48) Frisch, M. J.; Trucks, G. W.; Schlegel, H. B.; Scuseria, G. E.; Robb, M. A.; Cheeseman, J. R.; Scalmani, G.; Barone, V.; Mennucci, B.; Petersson, G. A.; Nakatsuji, H.; Caricato, M.; Li, X.; Hratchian, H. P.; Izmaylov, A. F.; Bloino, J.; Zheng, G.; Sonnenberg, J. L.; Hada, M.; Ehara, M.; Toyota, K.; Fukuda, R.; Hasegawa, J.; Ishida, M.; Nakajima, T.; Honda, Y.; Kitao, O.; Nakai, H.; Vreven, T.; Montgomery, J. A., Jr.; Peralta, J. E.; Ogliaro, F.; Bearpark, M.; Heyd, J. J.; Brothers, E.; Kudin, K. N.; Staroverov, V. N.; Kobayashi, R.; Normand, J.; Raghavachari, K.; Rendell, A.; Burant, J. C.; Iyengar, S. S.; Tomasi, J.; Cossi, M.; Rega, N.; Millam, J. M.; Klene, M.; Knox, J. E.; Cross, J. B.; Bakken, V.; Adamo, C.; Jaramillo, J.; Gomperts, R.; Stratmann, R. E.; Yazyev, O.; Austin, A. J.; Cammi, R.; Pomelli, C.; Ochterski, J. W.; Martin, R. L.; Morokuma, K.; Zakrzewski, V. G.; Voth, G. A.; Salvador, P.; Dannenberg, J. J.; Dapprich, S.;

Daniels, A. D.; Farkas, O.; Foresman, J. B.; Ortiz, J. V.; Cioslowski, J.; Fox, D. J. Gaussian 09, Revision C.01; Gaussian, Inc.: Wallingford CT, 2009.

[26] Chai, J.-D.; Head-Gordon, M. *Phys. Chem. Chem. Phys.*, **2008,** *10*, 6615–6620.

[27] Grimme, S.; Goerigk, L. *Phys. Chem. Chem. Phys.*, **2011,** *13*, 6670–6688.

[28] Chernichenko, K.; Madarász, Á.; Pápai, I.; Nieger, M.; Leskelä, M.; Repo, T. *Nat. Chem.* **2013**, *5*, 718-723.

[29] (a) Becke, A. D. *J. Chem. Phys.* **1993**, *98*, 5648–5652. (b) Burke, K. J.; Perdew, P.; Yang, W. *Electronic Density Functional Theory: Recent Progress and NewDirections*, (Ed: J. F. Dobson; G. Vignale, M. P. Das), Springer, Heildelberg, **1998.**

[30] (a) Francl, M. M.; Pietro, W. J.; Hehre, W. J.; Binkley, J. S.; Gordon, M. S.; Defrees, D. J.; Pople, J. A. *J. Chem. Phys.* **1982**, *77*, 3654-3665. (b) Hehre, W. J.; Ditchfield, R.; Pople, J. A. *J. Chem. Phys.***1972**, *56*, 2257-2261.

[31] Andrae, D.; Heussermann, U.; Dolg, M.; Stoll, H.; Preuss, H. *Theor. Chim. Acta.* **1990,** *77*, 123–141.

[32] Grimme, S. *J. Comp. Chem.* **2006**, *27*, 1787-1799.

[33] Marenich, A. V.; Cramer, C. J.; Truhlar, D. G. *J. Phys. Chem. B*, **2009,** *113*, 6378-6396.

[34] (a) Huang, D.; Makhlynets, O. V.; Tan, L. L.; Lee, S. C.; Rybak-Akimova, E. V.; Holm, R. H. *Inorg. Chem.* **2011**, *50*, 10070−10081. (b) Huang, D. G.; Makhlynets, O. V.; Tan, L. L.; Lee, S. C.; Rybak-Akimova, E. V.; Holm, R. H. *Proc. Natl. Acad. Sci. U. S. A.* **2011,** *108*, 1222−1227. (c) Zhang, C. G.; Zhang, R.; Wang, Z. X.; Zhou, Z.; Zhang, S. B.; Chen, Z. *Chem. Eur. J.* **2009**, *15*, 5910-5919. (d) Liang, Y.; Liu, S.; Xia, Y.; Li, Y.; Yu, Z. X. *Chem. Eur. J.* **2008,** *14*, 4361-4373. (e) Chen, Y.; Ye, S.; Jiao, L.; Liang, Y.; Sinha-Mahapatra, D. K.; Herndon, J. W.; Yu, Z.

X. *J. Am. Chem. Soc*. **2007,** *129*, 10773-10784. (f) Yu, Z. X.; Houk, K. N. *J. Am. Chem. Soc.* **2003**, *125*, 13825-13830.

[35] Liang, Y.; Liu, S.; Xia, Y. Z.; Li, Y. H.; Yu, Z. X. *Chem. Eur. J.* **2008,** *14*, 4361-4373.

[36] (a) Martin, R. L., Hay, P. J, Platt, L.R. *J. Phys. Chem. A*, **1998**, *102*, 3565-3573. (b) Siffert, N.; Buehl, M. *J. Am. Chem. Soc.*, **2010**, *132*, 8056-8070.

[37] Dimare, M. *J. Org. Chem.*, **1996**, *61*, 8378-8385.

[38] All attempts to isolate an intermediate where CO_2 was only coordinated to the phosphine moiety while being reduced by HBcat led to **TS1A**.

[39] (a) Corey, E. J.; Link, J. O. *Tet. Lett.* **1989**, *30*, 6275-6278. (b) Corey, E.J.; Bakshi, R. K. *Tet. Lett.* **1990**, *31*, 611-614.

[40] Westcott, S. A.; Blom, H. P., Marder, T. B.; Baker, R. T.; Calabrese, J. C. *Inorg. Chem.* **1993**, *32*, 2175-2182.

[41] Eisenberger, P.; Bailey, A. M.; Crudden, C. M. *J. Am. Chem. Soc.* **2012**, *134*, 17384-17387. Generation of the hydridoborate/boronium ion pair was also considered to occur through coordination to phosphine or from IM0A, but the TS were found to be higher (see ESI).

[42] Kabalka, G.W.; Baker, J. D.; Neal, G.W. *J. Org. Chem,* **1977**, *42*, 512-517.

[43] Lim, C. H.; Holder, A. M.; Hynes, J. T.; Musgrave, C. B. *Inorg.Chem.* **2013,** *52*, 10062-10066.

TOC graphic: